

# Remote Monitoring of Two-State Markov Sources via Random Access Channels: an Information Freshness vs. State Estimation Entropy Perspective

Giuseppe Cocco, *Senior Member, IEEE*, Andrea Munari, *Senior Member, IEEE*, Gianluigi Liva, *Senior Member, IEEE*

## Abstract

We study a system in which two-state Markov sources send status updates to a common receiver over a slotted ALOHA random access channel. We characterize the performance of the system in terms of state estimation entropy (SEE), which measures the uncertainty at the receiver about the sources' state. Two channel access strategies are considered, a *reactive* policy that depends on the source behaviour and a *random* one that is independent of it. We prove that the considered policies can be studied using two different hidden Markov models (HMM) and show through density evolution (DE) analysis that the reactive strategy outperforms the random one in terms of SEE while the opposite is true for AoI. Furthermore, we characterize the probability of error in the state estimation at the receiver, considering a maximum a posteriori (MAP) estimator and a low-complexity (decode & hold) estimator. Our study provides useful insights on the design trade-offs that emerge when different performance metrics such as SEE, age or information (AoI) or state

All authors contributed equally to this work. Part of the results in this paper will be presented at the IEEE Information Theory Workshop (ITW), April 23-28 2023, Saint-Malo, France.

G. Cocco is with the Signal Theory and Communications Department, Universitat Politècnica de Catalunya (UPC), Barcelona (Spain), and with the Department of Information and Communication Technologies, Universitat Pompeu Fabra. (email: giuseppe.cocco@upc.edu)

A. Munari and G. Liva are with the Institute of Communications and Navigation, German Aerospace Center (DLR), Wessling, Germany (email: {andrea.munari, gianluigi.liva}@dlr.de)

The work of G. Cocco was supported by the Ramon y Cajal fellowship program (grant RYC2021-033908-I) funded by MCIN/AEI/10.13039/501100011033 and by the European Union "NextGenerationEU" Recovery Plan for Europe, by the Secretary of Universities and Research (Catalan Government) under a Beatriu de Pinós fellowship, and by the European Union's Horizon 2020 research and innovation programme under the Marie Skłodowska-Curie grant agreement 801370.

A. Munari and G. Liva acknowledge the financial support by the Federal Ministry of Education and Research of Germany in the programme of "Souverän. Digital. Vernetzt." Joint project 6G-RIC, project identification number: 16KISK022.

estimation probability error are adopted. Moreover, we show how the source statistics significantly impact the system performance.

## I. INTRODUCTION

**M**ONITORING the state of remotely-deployed nodes in wireless sensor networks is one of the possible applications of Internet of Things (IoT) systems. Such use cases are typically characterized by the presence of a large number of battery-powered, low-complexity devices which sense an underlying process and send updates to a common receiver over a shared channel in an often sporadic and unpredictable fashion. In these settings, grant-based solutions that require channel negotiation and reservation procedures to allocate resources prior to data delivery tend to be highly inefficient, and uncoordinated access protocols based on variations of the well-known ALOHA scheme [1] are commonly employed to enable connectivity [2].

The main goal in remote-monitoring IoT applications is to maintain an accurate knowledge at the receiver of the status of the sensed processes. The task is in general not trivial, as it jointly depends on how nodes generate (relevant) readings, as well as on the latency experienced by sent packets in the network, and it becomes especially challenging in the presence of a distributed channel contention.

Important steps towards characterizing the problem were taken with the definition of some relevant performance indicators. A pioneering role in this sense was played by the age of information (AoI), originally introduced in [3][4], in the context of vehicular communications. The metric is defined as the time elapsed since the generation of the last received update for a process of interest, and captures how fresh the knowledge available at the receiver is. By virtue of its usefulness and mathematical tractability, AoI has received a lot of research attention [5], allowing to identify some fundamental trade-offs and protocol design principles that depart from those obtained using classical metrics such as throughput or latency. While initial works focused on point-to-point links, e.g. [6]–[10] among the vast available literature, important results were recently obtained also for multiple sources [11]–[16], providing fundamental insights on the behavior under ALOHA-based contention [17]–[20].

By definition, AoI is oblivious of the content of status updates being sent, focusing only on the time of their generation, and defines a penalty that continues to grow in the absence of new incoming messages even if the monitored process does not change its state. As such, the metric may fall short in accurately capturing the uncertainty experienced at the receiver, especially in the presence of non-memoryless sources. To overcome this limitation, alternative

performance indicators have recently been proposed, such as age of incorrect information [21] or value of information [22]. In the first case, a (possibly non-linear) penalty is undergone only if the estimate available at the receiver is not sufficiently precise (e.g., it differs from the actual state of the source). Similarly, value of information aims at measuring the relevance of received updates towards improving the estimate of a process for a specific task. In this context, a metric of particular interest is the state estimation entropy (SEE) [23], which quantifies the uncertainty in the knowledge of the sources' state at the sink, based on current and past channel outputs as well as on the source model. From this standpoint, while recent results were obtained in scheduled multi-user setups [24], [25], the behavior in random access systems is still largely unexplored.

In this paper, we provide a contribution in this direction by detailing and extending the initial analysis presented in [26]. In particular, we consider a system in which nodes monitoring two-state Markov sources communicate towards a common receiver over a slotted ALOHA channel without feedback. Under the assumption of destructive collisions, we investigate the ability of the system to acquire accurate estimates of the state of the sources at the receiver leaning on SEE. We consider two variations of the ALOHA access: a random transmission strategy, where the nodes send updates of their state with a fixed probability in each slot according to a Bernoulli process, and a reactive transmission strategy, where an update is sent only when a change of state in the underlying Markov source is detected. Our study reveals that the latter approach can drastically reduce the SEE, highlighting the importance of an access strategy that is tuned to the process being monitored. Notably, this result is in contrast to what suggested when AoI is considered as the metric of reference, in which case a random transmission approach tuned to achieve throughput maximization is optimal also in the AoI sense for ALOHA channels [27], [28]. The intuition underlying this discrepancy follows the observation that, when the value of the monitored process is relevant, reporting only state changes can help in reducing congestion, favoring delivery of informative updates to the receiver.

The key contributions of the present work can be summarized as follows:

- We provide an analytical characterization of the SEE for both the random and the reactive transmission strategies. In particular, we show that these approaches can be modeled using two distinct hidden Markov models. Moreover, we provide an efficient evaluation of their SEE via a density evolution analysis [29][30, Chapter 4], with a complexity that grows only quadratically in the number of nodes.
- Leaning on this, we study the behavior of the access schemes in the case of both

symmetric and asymmetric sources (i.e., with different transition probabilities between the two available states). In the latter case, we propose an approximated model to simplify the DE analysis, and show by means of simulations that it provides a tight match in terms of the SEE. Comparing the trends obtained for SEE and average AoI, the trade-offs induced by a reactive transmission approach are thoroughly discussed. From this standpoint, our work provides some useful hints for protocol design in IoT monitoring systems.

- For both transmission strategies, we also study the state estimation error probability achieved by a MAP estimator and by a simpler solution, dubbed decode and hold (D&H), which only updates the state estimate upon successfully receiving a message informing the receiver about the state of the tracked source. Our analysis shows that the D&H approach offers performance comparable to that of a MAP estimator when symmetric sources are monitored, whereas it exhibits a significant gap in the asymmetric case.

#### A. Related Works

The monitoring of one or more sources through an unreliable channel has received relevant research attention.

In the context of point-to-point channels, several works approached the problem of estimating the state of a single source. Among them, [9] studies the optimal sampling strategy that minimizes the mean square estimation error of a Wiener process under a sampling rate constraint, considering transmissions that incur queuing delay, and highlighting ties with an AoI-based optimization under specific conditions. In turn, [31] proposes an optimal transmission policy for a single sensor observing a stochastic source and transmitting the observation through a noisy channel. The considered approach takes into account past observations and decisions of the sensor, showing that a threshold-in-threshold policy is optimal under some conditions. Joint sampling and transmission strategies for  $N$ -state Markov sources are tackled [32], taking into account performance metrics such as the estimation error probability and the cost that an estimate error might have on actuation. Scheduling policies in a battery-constrained energy harvesting monitoring system are studied in [33] for Markov as well as Gaussian sources under different estimation distortion metrics.

Interesting results were recently derived also in multiple-access settings. In [34] a random access system with feedback in which each transmitter observes a different source, modelled as a random walk process, is studied. The Authors consider two possible strategies: an oblivious one – akin to the our random transmission approach – and a non-oblivious one,

which triggers a transmission only when the discrepancy between the current source value and the knowledge at the receiver exceeds a threshold. AoI and a weighted sum of the squared estimation errors are employed to evaluate the policies. In [35] a wireless sensor network is studied using the SEE as the loss function to be minimized through optimal scheduling. A similar setup is also considered in [36]. Important contributions were provided lately in [24], [25], where the Authors investigate a system that monitors multiple binary Markov processes. Studying the uncertainty of information (UoI), i.e. the entropy of a tracked process conditioned on the latest observation, the minimization of the average sum UoI is cast onto a restless multi-armed bandit problem, deriving optimal scheduling strategies. In [37] the Authors study the problem of remote estimation of a discrete-time linear dynamical source observed by multiple sensors that access a common receiver through a random access channel. In such work the trade-off between the number of transmitting nodes and the estimation accuracy is studied. Other works [38], [39] consider the problem of estimating the entropy rate of a hidden Markov model.

Going beyond these works, our contribution focuses on the performance at system level of different sampling strategies in terms of state estimation entropy, AoI and state estimation error in uncoordinated multiple access systems. We consider generic, i.e., not necessarily symmetric, underlying Markov sources and study the interaction between the sampling/channel access policy and the estimation entropy.

The remainder of the paper is organized as follows. Sec. II introduces the system model and the considered metrics. In Sec. III we discuss the optimal state estimation approach, describing the hidden Markov models for both the random and the reactive strategies, whereas a density evolution approach to efficiently evaluate their performance is presented in Sec. IV. Sec. V studies the state estimation error probability in the MAP and D&H case, followed by numerical results and discussion in Sec. VI, and by some concluding remarks in Sec. VII.

## II. SYSTEM MODEL AND PRELIMINARIES

### A. Notation

We use capital letters for random variables (r.v.s), and lower case letters for their realizations. The probability of an event  $\{X = x\}$  is denoted as  $P[X = x]$ , and the probability distribution function of the r.v.  $X$  as  $P(x) = P[X = x]$ . For finite state Markov chains, we denote the one-step transition probability from state  $i$  to state  $j$  as  $q_{ij}$ , and the stationary probability of state  $i$  as  $\pi_i$ .

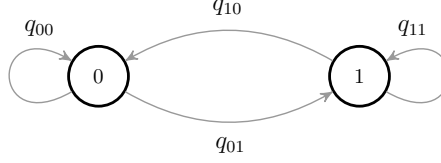


Fig. 1. Two-state Markov model for a generic source in the system.

### B. System Model

Throughout our discussion, we focus on a system with  $M$  statistically independent sources (nodes) that share a common wireless channel towards a receiver. Time is slotted, and all nodes are assumed to be slot-synchronized. The generic source  $k \in \{0, 1, \dots, M - 1\}$  generates a random sequence of symbols

$$X_0^{(k)} X_1^{(k)} X_2^{(k)} \dots$$

where  $X_n^{(k)}$  belongs to the alphabet  $\mathcal{X} = \{0, 1\}$ , and represents the (random) state of the source at time (slot index)  $n$ . Each node is modelled as a two-state stationary Markov chain with transition probabilities  $q_{ij} = \mathbb{P} \left[ X_n^{(k)} = j \mid X_{n-1}^{(k)} = i \right]$  for all  $(i, j) \in \mathcal{X} \times \mathcal{X}$ , as reported in Fig. 1. We denote the steady-state distribution of the process as

$$\begin{aligned} \pi_0 &= \frac{q_{10}}{q_{10} + q_{01}} \\ \pi_1 &= \frac{q_{01}}{q_{10} + q_{01}}. \end{aligned}$$

Every node in the network can transmit update packets over the shared channel, reporting information on the state of its source to the receiver. In this work we focus on random access medium sharing policies, commonly employed in practical settings, and consider two variations of the slotted ALOHA protocol [1] presented in details in Sec. II-C. Accordingly, three possible slot outcomes can be seen at the receiver: i) *idle*, i.e., no transmission is performed; ii) *singleton*, i.e., only one source has transmitted; iii) *collision*, i.e., two or more packets were sent concurrently. In the remainder, we assume the well-known collision channel model [1], so that the content of a status update is correctly received whenever sent over a singleton slot, whereas no packet can be decoded in the presence of a collision.

We further make some additional assumptions inspired by practical systems. First, we consider that the receiver is able to detect a collision when it takes place but does not have knowledge of the number of involved packets. Second, each transmission contains an

identifier of the source, and the receiver becomes aware of the current value of a process upon decoding a packet from the corresponding source. Finally, no feedback is provided, so that a node is not aware of the outcome of its delivery attempt, nor can estimate the current channel load. Accordingly, no retransmissions are performed, and an update is only sent once.<sup>1</sup>

Without loss of generality, we consider as reference the source with index  $k = 0$  and drop the superscript in  $X_n^{(k)}$ . Thus, the sequence of symbols generated by the reference source will be denoted by

$$X_0 X_1 X_2 \dots$$

and the receiver observes the random output sequence

$$Y_0 Y_1 Y_2 \dots$$

where  $Y_n$  belongs to the alphabet  $\mathcal{Y} = \{0, 1, \text{I}, \text{C}, \ominus, \oplus\}$ . Here, 0 and 1 denote a collision-free observation of the corresponding state of the reference source, I denotes an idle slot, C denotes a collision, and  $\ominus, \oplus$  denote a collision-free observation of the state of any of the other sources (with index in  $\{1, \dots, M-1\}$ ), where  $\ominus$  represents the “zero” state and  $\oplus$  the “one” state.

### C. Transmission Strategies

In the remainder of our study we compare two distinct transmission strategies. In spite of their simplicity, their analysis allows to capture some fundamental trade-offs of the considered system, providing relevant insights.

**Random transmission strategy:** In the first approach, each source randomly decides at each slot whether to transmit a status update, with *activation probability*  $\alpha$ , or to remain silent, with probability  $1 - \alpha$ . The decision is made independently of the evolution of the source process, as well as across slots. We will refer to this approach as *random transmission strategy*. In this case, the number of nodes accessing the channel over a slot follows a binomial distribution of parameters  $M$  and  $\alpha$ . Accordingly, the probability for the reference source to deliver an update at time  $n$  is given by

$$\omega = \alpha(1 - \alpha)^{M-1} \quad (1)$$

<sup>1</sup>This setup is commonly employed in many practical IoT systems, e.g. LoRaWAN [2], where sensing tasks are performed by simple, battery-powered nodes that operate without feedback from the receiver.

capturing the probability that a message is transmitted and does not undergo a collision.

**Reactive transmission strategy:** The second approach we tackle foresees a terminal access the channel over a slot only if a state change in the corresponding source takes place. Otherwise, no transmission is performed. For such solution, referred to as *reactive transmission strategy*, the probability for a source to deliver an update over a generic slot can be approximated as

$$\omega \simeq \tilde{\alpha} (1 - \tilde{\alpha})^{M-1} \quad (2)$$

where

$$\tilde{\alpha} := \pi_0 q_{01} + \pi_1 q_{10} = \frac{2q_{01}q_{10}}{q_{01} + q_{10}} \quad (3)$$

is an estimate of the activation probability for a node. The formulation is exact in the symmetric case  $q_{01} = q_{10}$ , and only provides an approximation otherwise. Indeed, when  $q_{01} \neq q_{10}$ , the behavior of a node across subsequent slots is no longer i.i.d, as it depends on the current state of the source. Further details on this approximation will be discussed in Sec. III-D1, showing that, in spite of its simplicity, it leads to very accurate estimates of the metrics of interest. Incidentally, note that, under the reactive strategy, the access probability is fully determined by the source statistics.<sup>2</sup>

We also remark that this policy triggers a key trade-off. On the one hand, avoiding transmission of state information if no change at the source is observed may reduce the channel congestion, with beneficial effects on the overall packet delivery probability. On the other hand, the unavoidable collisions in a random access setting entail the risk of not providing updates for a long time when the source rarely changes state. In addition, it is important to observe how collisions or idle slots carry information about the state of the sources, as the access strategy intrinsically depends on whether the tracked processes experience a transition.

#### D. State Estimation Entropy and Error Probability

Let us denote by  $Y^n$  the random vector containing the output sequence from 0 to the current time  $n$ , and by  $y^n$  its realization. The uncertainty experienced at the receiver about

<sup>2</sup>To attain more flexibility, one may conceive modified (randomized) reactive transmission strategies, where the access probability may be tuned by introducing a probability of transmission in presence of a state change (to lower the channel load) or a probability to perform additional transmissions even in absence of state change. These modifications will not be considered in this work.

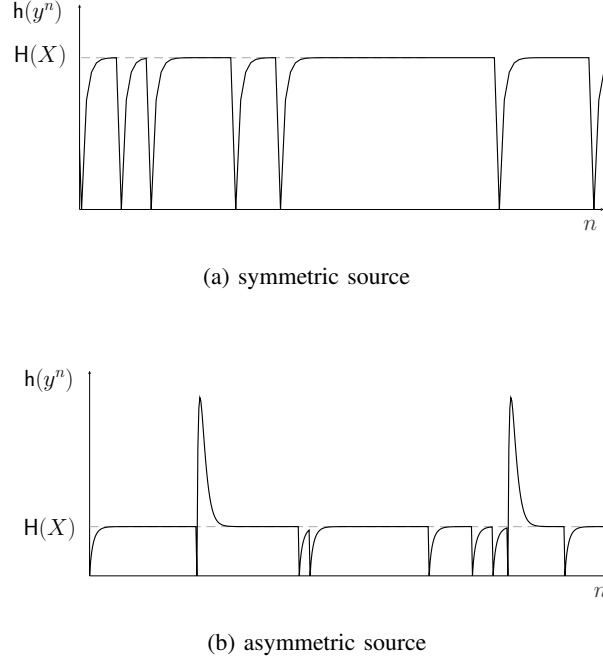


Fig. 2. Example of time evolution of  $h(y^n)$  for a single source implementing a random transmission policy. The metric is reset to a zero whenever an update is delivered, and converges to the entropy of the source,  $H(X)$ , when the receiver does not obtain any information for long periods of time. (a) reports the case of a symmetric source ( $q_{01} = q_{10}$ ), whereas (b) shows the behavior of an asymmetric source ( $q_{01} \neq q_{10}$ ).

the present state of the monitored source can be conveniently captured by the entropy<sup>3</sup>

$$\begin{aligned} h(y^n) &:= H(X_n | Y^n = y^n). \\ &= E[\log P[X_n | Y^n = y^n]] \end{aligned} \quad (4)$$

where the expectation is taken with respect to the conditioned variable  $X_n$ .

**Example 1.** To get preliminary insights on this metric, consider the case of a single source in the absence of channel contention (i.e.,  $M = 1$ , no collisions). The node follows the random transmission policy, sending (successful) updates with a certain probability at every slot. An example of the evolution over time of  $h(y^n)$  for a symmetric source ( $q_{01} = q_{10}$ ) is reported in Fig. 2a, showing how the uncertainty grows until an update is received, when a reset to zero denotes exact knowledge acquired at the receiver on the status of the tracked source. Note that, in the absence of refreshes,  $h(y^n)$  approaches the entropy of the stationary distribution of the source  $H(X) = -\pi_0 \log_2 \pi_0 - \pi_1 \log_2 \pi_1$ . The situation changes for an asymmetric source, as illustrated in Fig. 2b for the case  $q_{10} = 0.2$  and  $q_{01} = 0.01$ , corresponding to a

<sup>3</sup>The notation  $h(\cdot)$  should not be confused with the one that is sometimes used for differential entropy.

stationary distribution  $\pi_0 = 0.047$ ,  $\pi_1 = 0.953$ . Note indeed that, when an update is delivered informing that the source is in state 1,  $h(y^n)$  grows slowly, in view of the low probability of state transition. Conversely, if the receiver is informed that  $X$  has reached state 1, a higher uncertainty follows in the subsequent slots, progressively reducing to converge to  $H(X)$  in the absence of updates. In the example, the probability of the source being in state 1 decreases from  $P(1) = 1$  right after an update is received, to around  $P(1) = 0.517$  after only three slots, with a corresponding increase in uncertainty about the source state.

Two further remarks are in order. We first observe that, for the single source case,  $h(y^n)$  is identically 0 when a reactive transmission strategy is implemented, as the receiver can perfectly track the state of the source. Second, it is to be pointed out that the behavior of the metric becomes more involved when multiple nodes contend for the channel. In this case, the uncertainty on the tracked source varies differently based on the outcomes observed over the slots, as well as on the implemented transmission strategy. More details will be discussed in the following sections.

To characterize the performance of the transmission strategies we aim at deriving the distribution of the r.v.

$$H_n := h(Y^n) \quad (5)$$

and, in particular, its mean value  $E[H_n] = H(X_n|Y^n)$ . More specifically, we are interested in the evaluation of the limiting behavior of such quantity as  $n \rightarrow \infty$ , denoted as  $H_\infty$  and referred to as *average state estimation entropy*. We also note that  $H_\infty$  coincides with the time average

$$\lim_{N \rightarrow \infty} \frac{1}{N} \sum_{n=0}^{N-1} H(X_n|Y^n).$$

This follows by observing that  $(X_n, Y_n)$  is a stationary stochastic process, hence  $H(X_n|Y^n)$  is monotonically non-increasing and converges to a limit. The limit coincides with  $H_\infty$  by the Cesàro mean Theorem [40, Theorem 4.2.3].

In the remainder, we also tackle the problem of estimating the reference source state at the receiver. In this context, consider a generic state estimator for  $X_n$ , and denote the estimate as  $\hat{X}_n$ . We introduce the state estimation error probability at time  $n$  as

$$P_e^{(n)} = P[\hat{X}_n \neq X_n]$$

and denote by

$$P_e = \lim_{N \rightarrow \infty} \frac{1}{N} \sum_{n=0}^{N-1} P_e^{(n)} \quad (6)$$

the time average of the sequence  $P_e^{(n)}$ .

### E. Age of Information

As a reference benchmark for our study, we study the performance of the presented schemes in terms of AoI. The metric, originally introduced in [41], is a well-established measure for the notion of information freshness, capturing how outdated the knowledge about the state of a source is at the destination. To introduce this quantity, we assume each status update to contain a time stamp, denoting the instant at which the message was generated. Accordingly, the current AoI for the source of interest at time  $t$  is defined as

$$\Delta(t) := t - \sigma(t)$$

where  $\sigma(t)$  is the time stamp of the last successfully received update from the node. Leaning on this definition,  $\Delta(t)$  follows a sawtooth profile, growing linearly over time and being reset each time an update is received as exemplified in Fig. 3. For the setting under study, we assume that the time stamp of a message corresponds to the the start of that slot it is sent over, so that the AoI falls to one slot duration if the packet is successfully decoded, accounting for the transmission and reception time of the message over the channel. Via simple arguments, the stochastic process  $\Delta(t)$  can be shown to be ergodic (see, e.g. [42]), and we will focus in the remainder on its average value

$$\bar{\Delta} := \mathbb{E}[\Delta(t)] = \lim_{N \rightarrow \infty} \frac{1}{N} \sum_{n=0}^{N-1} \Delta(n)$$

where  $n = \lfloor t \rfloor$ . For a slotted ALOHA access, assuming independent behavior of all nodes across slots,  $\bar{\Delta}$  takes the simple form [42]

$$\bar{\Delta} = \frac{1}{2} + \frac{1}{\omega}. \quad (7)$$

where  $\omega$  is given for the random and reactive transmission strategies in (II-C) and (II-C), respectively. Note that, from (II-E), the metric is minimized by maximizing  $\omega$ . In other words, the optimal strategy in terms of AoI coincides, for a slotted ALOHA access, with a throughput maximization.

## III. EFFICIENT OPTIMUM STATE ESTIMATION

As a first step towards characterizing the performance of the system under study, we address the problem of estimating the state  $X_n$  of the reference source at the receiver upon observing a sequence of channel outputs  $y^n$ . In particular, we lean on the a-posteriori probability (APP) logarithmic ratio

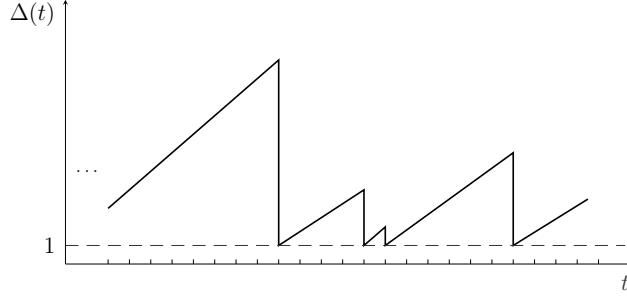


Fig. 3. Example of time evolution of age of information for a source of interest at the destination. The metric is reset to a value of one slot whenever an update is received, and grows linearly otherwise.

$$\lambda_n := \ln \frac{\mathbb{P}[X_n = 0 \mid Y^n = y^n]}{\mathbb{P}[X_n = 1 \mid Y^n = y^n]} \quad (8)$$

which, combined with a threshold test ( $\hat{x}_n = 0$  if  $\lambda_n > 0$  and  $\hat{x}_n = 1$  otherwise), yields an optimum maximum a posteriori (MAP) estimator, i.e., an estimator that minimizes the state estimation error probability.

In the remainder of this section, we introduce hidden Markov models to capture the relation between the observed channel outputs and the evolution of the reference source, and use them to develop recursive equations to efficiently compute (III). To this aim, we also show that the APP is a sufficient statistics for  $X_n$ . The results will be used in Sec. IV to derive the distribution of the distribution of the r.v.  $H_n$  and eventually the average state estimation entropy.

#### A. Hidden Markov Models

The statistical relation between the output sequence  $Y^n$  and the reference source sequence  $X^n$  can be suitably described via different hidden Markov models (HMMs), depending on the transmission strategy adopted by the nodes.

*1) Random Transmission Strategy:* In this case, the observation of channel outputs in  $\{\ominus, \oplus\}$  can be assimilated to the observation of an idle slot, i.e., the knowledge of the state of the other sources does not provide information about the state of the reference source (we will see that this is not true for other transmission policies). From this and the memoryless

nature of the access strategy, it follows that the statistical relation between the output sequence  $Y^n$  and  $X^n$  is fully characterized by the conditional probability function

$$P(Y^n|X^n) = \prod_{\ell=0}^n P(y_n | x_n). \quad (9)$$

The distribution in (III-A1) can readily be derived leaning on the activation probability of the nodes, as well as of the underlying Markov process  $X^n$ , as detailed in Appendix A.

2) *Reactive Transmission Strategy*: In this case the observation of channel outputs in  $\{\ominus, \oplus\}$  should be used to refine the estimate of the state of the reference source. To see why this is true, let us consider the following example.

**Example 2.** Assume the case  $M = 3$  with sources being driven by the transition probabilities  $q_{00} = 0.1$ ,  $q_{01} = 0.9$ ,  $q_{10} = 0.1$ , and  $q_{11} = 0.9$ . Note that a state change, hence a transmission, is much more probable if the past state is 0. The observation at time  $n - 1$  is  $Y_{n-1} = 0$  (the past state of the reference source is 0), whereas a collision is experienced at slot  $n$ , i.e.  $Y_n = \mathbf{C}$ . Consider the following different situations for the other two sources at time  $n - 1$ :

- a)  $X_{n-1}^{(1)} = 0$  and  $X_{n-1}^{(2)} = 0$ ;
- b)  $X_{n-1}^{(1)} = 1$  and  $X_{n-1}^{(2)} = 1$ .

In case (a), all three sources have the same probability of transition to a different state at time  $n$ , and hence of generating a transmission in slot  $n$ . It follows that the reference source participates in the collision on slot  $n$  (as a consequence of a state change) with probability  $1 - q_{00}/(3q_{00} + q_{01}) \approx 0.91$ . This can be checked by counting the fraction of “configurations” of transmission events yielding a collision. In case (b), the same probability is  $1 - q_{00}q_{10}/(2q_{00}q_{11} + q_{01}q_{10} + q_{00}q_{10}) \approx 0.97$ .

From the example above we can see that, under reactive sampling, having (even partial) knowledge of the state of the other sources, jointly with the channel output observations, provides information on the state of the reference source. From a careful inspection of the example we also see that what matters is not the state of each source, but rather the number of sources that are in a given state during the past slot. Accordingly, we denote by  $S_n$  the r.v. that counts the number of sources (with the exclusion of the reference one) that are in state 0 at time  $n$ . Obviously,  $S_n \in \mathcal{S}$  with  $\mathcal{S} = \{0, 1, \dots, M - 1\}$ . For the sake of estimating the state of the reference source, the system can be characterized as a stationary  $2M$ -state Markov chain  $\sigma_n := (X_n, S_n)$ , with state space  $\mathcal{X} \times \mathcal{S}$ . The channel output depends on the

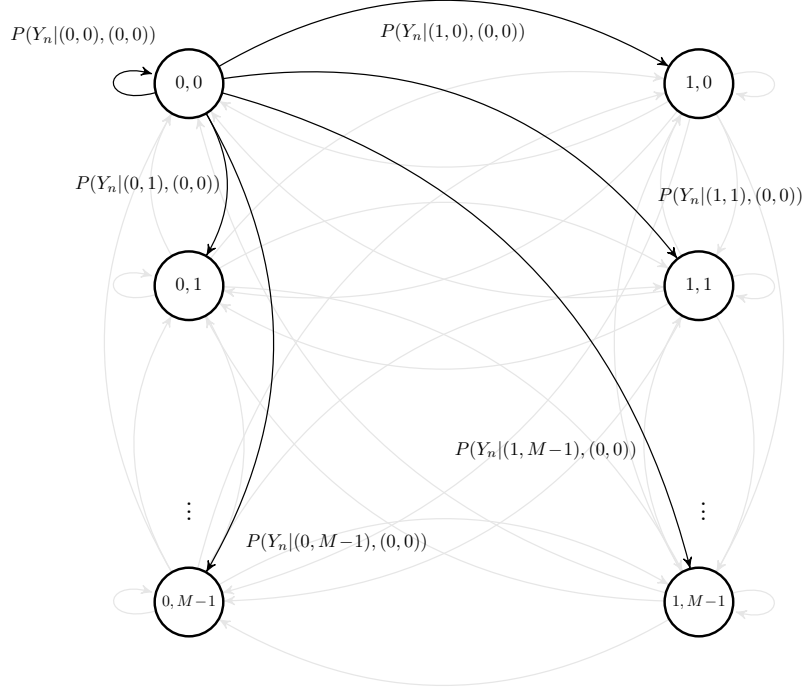


Fig. 4. Hidden Markov model for the reactive transmission strategy. The underlying Markov chain has state  $\sigma_n = (X_n, S_n)$ , where  $S_n$  denotes the number of nodes, other than the tracked source, that are in state 0 at time  $n$ . The observed outputs depend on the system state through the conditional probabilities  $P(y_n | \sigma_{n-1}, \sigma_n)$ , some of which are highlighted in the diagram.

system state transition through the conditional probability function  $P(y_n | \sigma_{n-1}, \sigma_n)$ , leading to the HMM illustrated in Fig. 4.

**Remark 1.** Note that, when  $q_{01} = q_{10}$  (symmetric sources), the information on the counter  $S_n$  can be dropped without any information loss, as the knowledge of  $S_n$  does not influence the probability of observing a collision at step  $n+1$ . In this case, the conditional probability function  $P(y_n | x_{n-1}, x_n)$  suffices, and the HMM simplifies to the one reported in Fig. 5.

### B. A-Posteriori Probability Logarithmic Ratio

Let us now further elaborate on the APP logarithmic ratio introduced in (III). First, we provide the following lemma to show that  $\lambda_n$  is a sufficient statistic for  $X_n$ .

**Lemma 1.** Assume  $X_0, X_1, \dots$  to be the random sequence of states generated by a two-state stationary Markov source, and let  $Y_0, Y_1, \dots$  be the state sequence observations. Then,  $\lambda_n$  is a sufficient statistic for estimating  $X_n$  given  $Y^n$ .

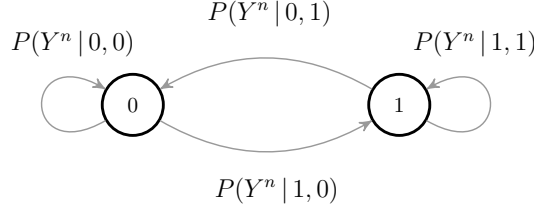


Fig. 5. Hidden Markov model for the reactive transmission policy, when symmetric sources are observed ( $q_{01} = q_{10}$ ).

*Proof.* Leaning on the Fisher-Neyman factorization theorem, it suffices to show that  $P(y^n|x_n)$  can be factored as  $a(x_n, \lambda_n) b(y^n)$ ,  $a(\cdot)$  and  $b(\cdot)$  being non-negative functions. Following [43, Lemma 4.7], we observe that

$$\ln \frac{P(x_n | y^n)}{P[X_n = 0 | Y^n = y^n]} = \begin{cases} 0 & \text{if } x_n = 0 \\ -\lambda_n & \text{if } x_n = 1 \end{cases}$$

which implies that

$$P(x_n|y^n) = P[X_n = 0 | Y^n = y^n] \exp(-x_n \lambda_n).$$

By Bayes' rule, we then have

$$P(y^n|x_n) = \frac{P(x_n|y^n)P(y^n)}{P(x_n)} = \frac{P[X_n = 0 | Y^n = y^n] \exp(-x_n \lambda_n) P(y^n)}{P(x_n)} = a(x_n, \lambda_n) b(y^n)$$

where  $a(x_n, \lambda_n) = \exp(-x_n \lambda_n)/P(x_n)$  and  $b(y^n) = P[X_n = 0 | Y^n = y^n] P(y^n)$ .  $\square$

Lemma 1 allows to characterize the distribution of the r.v.  $H_n$  defined in (II-D). Note indeed that  $X_n \rightarrow \Lambda_n \rightarrow Y^n$ , i.e., they form a Markov chain. Leaning on this, we have

$$\lambda_n = \ln \frac{P[X_n = 0 | \Lambda_n = \lambda_n]}{P[X_n = 1 | \Lambda_n = \lambda_n]}$$

where  $P[X_n = x_n | \Lambda_n = \lambda_n] = \exp(-x_n \lambda_n)/(1 + \exp(-\lambda_n))$ . By the data processing inequality, (II-D) can be written in terms of the APP logarithmic ratio as [40, Chapter 2]

$$\begin{aligned} h(y^n) &= H(X_n | Y^n = y^n) = H(X_n | \Lambda_n = \lambda_n) \\ &= \sum_{x_n=0}^1 \frac{\exp(-x_n \lambda_n)}{1 + \exp(-\lambda_n)} \log_2 \left( \frac{1 + \exp(-\lambda_n)}{\exp(-x_n \lambda_n)} \right). \end{aligned} \tag{10}$$

With a slight abuse of notation, we denote the leftmost term of (III-B) as  $h(\lambda_n)$ .

**Remark 2.** By observing that  $H_n = h(\Lambda_n)$  we see that the distribution of the r.v.  $H_n$  can be derived from the distribution of the APP logarithmic ratio  $\Lambda_n$ .

We now focus on deriving a recursive formulation to obtain the APP logarithmic ratio  $\lambda_n$  as a function of its previous value  $\lambda_{n-1}$  and of the channel observation  $y_n$ , for both the random and reactive transmission strategies.

### C. Random Transmission Strategy

By Bayes' theorem we can rewrite (III) as

$$\lambda_n = \ln \frac{P[X_n = 0, Y^n = y^n]}{P[X_n = 1, Y^n = y^n]}. \quad (11)$$

Observe that

$$P(x_n, y^n) = P(y_n | x_n) \sum_{x_{n-1}=0}^1 P(x_n | x_{n-1}) P(x_{n-1}, y^{n-1}) \quad (12)$$

where the result follows from well-known steps for the derivation of the forward-backward algorithm recursions over HMMs (see e.g. [44], [45]). By using (III-C) in (III-C) we obtain

$$\begin{aligned} \lambda_n &= \ln \frac{\sum_{x_{n-1}=0}^1 P[X_n = 0, X_{n-1} = x_{n-1}, Y^{n-1} = y^{n-1}, Y_n = y_n]}{\sum_{x_{n-1}=0}^1 P[X_n = 1, X_{n-1} = x_{n-1}, Y^{n-1} = y^{n-1}, Y_n = y_n]} \\ &\stackrel{(a)}{=} \ln \frac{\sum_{x_{n-1}=0}^1 P[X_n = 0, Y_n = y_n | X_{n-1} = x_{n-1}] P(x_{n-1} | y^{n-1})}{\sum_{x_{n-1}=0}^1 P[X_n = 1, Y_n = y_n | X_{n-1} = x_{n-1}] P(x_{n-1} | y^{n-1})} \\ &\stackrel{(b)}{=} \ln \frac{P(y_n | 0)}{P(y_n | 1)} + \ln \frac{\sum_{x_{n-1}=0}^1 P[X_n = 0 | X_{n-1} = x_{n-1}] P(x_{n-1} | \lambda_{n-1})}{\sum_{x_{n-1}=0}^1 P[X_n = 1 | X_{n-1} = x_{n-1}] P(x_{n-1} | \lambda_{n-1})} \\ &\stackrel{(c)}{=} \ln \frac{P(y_n | 0)}{P(y_n | 1)} + \ln \frac{q_{00} + q_{10} \exp(-\lambda_{n-1})}{q_{01} + q_{11} \exp(-\lambda_{n-1})} \\ &=: f(y_n, \lambda_{n-1}). \end{aligned} \quad (13)$$

In (III-C), (a) follows by Bayes' Theorem and by observing that  $(X_n, Y_n)$  are independent on  $Y^{n-1}$  once we condition on  $X_{n-1}$ . Similarly, (b) follows by application of Bayes' Theorem and by observing that  $Y_n$  is independent on  $X_{n-1}$  once we condition on  $X_n$ . Moreover, since  $\lambda_{n-1}$  is a sufficient statistic for  $x_{n-1}$ , we can replace  $P(x_{n-1} | y^{n-1})$  with  $P(x_{n-1} | \lambda_{n-1})$ . Finally, (c) is obtained by introducing the Markov source transition probabilities, and by noting that  $P(x_{n-1} | \lambda_{n-1}) \propto \exp(-x_{n-1} \lambda_{n-1})$ . The recursion is hence defined via  $\lambda_n = f(y_n, \lambda_{n-1})$ , and its evaluation complexity is independent on the number of sources.

#### D. Reactive Transmission Strategy

In the reactive case, the derivation of the APP logarithmic ratio is based on the recursive computation of the state probabilities for the  $2M$ -states HMM described in Section III-A2. Following the steps of the forward-backward algorithm recursions, we have:

$$\begin{aligned}
 P(\sigma_n, y^n) &\stackrel{(a)}{=} \sum_{\sigma_{n-1} \in \mathcal{X} \times \mathcal{S}} P(\sigma_n, \sigma_{n-1}, y_n, y^{n-1}) \\
 &\stackrel{(b)}{=} \sum_{\sigma_{n-1} \in \mathcal{X} \times \mathcal{S}} P(\sigma_n, y_n | \sigma_{n-1}, y^{n-1}) P(\sigma_{n-1}, y^{n-1}) \\
 &\stackrel{(c)}{=} \sum_{\sigma_{n-1} \in \mathcal{X} \times \mathcal{S}} P(y_n | \sigma_{n-1}, \sigma_n) P(\sigma_n | \sigma_{n-1}) P(\sigma_{n-1}, y^{n-1}). \tag{14}
 \end{aligned}$$

In (III-D), (a) follows from the law of total probability, (b) from straightforward application of Bayes' Theorem, and (c) by exploiting the Markov property. At every step, the APP logarithmic ratio can be evaluated as

$$\lambda_n = \ln \frac{\sum_{\sigma_n \in \{0\} \times \mathcal{S}} P(\sigma_n, y^n)}{\sum_{\sigma_n \in \{1\} \times \mathcal{S}} P(\sigma_n, y^n)}.$$

We remark that the complexity of the calculation entailed by the recursion grows quadratically with the number of states in the HMM, i.e., the complexity grows with  $M^2$ . We describe in the following a sub-optimal algorithm that computes approximate values of the APP logarithmic ratios with a complexity that is independent on the number of sources. This makes it suited in cases in which  $M$  is large.

1) *Myopic State Estimation*: The recursive calculation implementing the optimal detector requires tracing probabilities over a trellis diagram with  $2M$  states. A simplified approach consists in neglecting the effect of  $S_{n-1}$  and  $S_n$  on the probability of observing  $Y_n$ . This is equivalent to the derivation of a recursive state estimator where (a) the reference source adopts a reactive transmission approach and (b) all the remaining  $M - 1$  sources adopt a random transmission one with  $\alpha$  set to the stationary probability of a state change  $\tilde{\alpha} := \pi_0 q_{01} + \pi_1 q_{10}$ . We refer to the estimator obtained under this approximation as *myopic estimator*, and to the model described by conditions (a) and (b) as *surrogate myopic model*.

For such model we have  $P(y_n | \sigma_n, \sigma_{n-1}) = P(y_n | x_n, x_{n-1})$ , hence

$$P(x_n, y^n) = \sum_{x_{n-1}=0}^1 P(y_n | x_n, x_{n-1}) P(x_n | x_{n-1}) P(x_{n-1}, y^{n-1}) \tag{15}$$

resulting in the myopic APP logarithmic ratio recursion

$$\begin{aligned}
\tilde{\lambda}_n &= \ln \frac{\sum_{x_{n-1}=0}^1 \mathbb{P}[X_n = 0, X_{n-1} = x_{n-1}, Y^{n-1} = y^{n-1}, Y_n = y_n]}{\sum_{x_{n-1}=0}^1 \mathbb{P}[X_n = 1, X_{n-1} = x_{n-1}, Y^{n-1} = y^{n-1}, Y_n = y_n]} \\
&\stackrel{(a)}{=} \ln \frac{\sum_{x_{n-1}=0}^1 \mathbb{P}[Y_n = y_n | X_{n-1} = x_{n-1}, X_n = 0] \mathbb{P}[X_n = 0 | X_{n-1} = x_{n-1}] P(x_{n-1} | y^{n-1})}{\sum_{x_{n-1}=0}^1 \mathbb{P}[Y_n = y_n | X_{n-1} = x_{n-1}, X_n = 1] \mathbb{P}[X_n = 1 | X_{n-1} = x_{n-1}] P(x_{n-1} | y^{n-1})} \\
&\stackrel{(b)}{=} \ln \frac{\sum_{x_{n-1}=0}^1 \mathbb{P}[Y_n = y_n | X_{n-1} = x_{n-1}, X_n = 0] q_{x_{n-1}0} \exp(-x_{n-1} \tilde{\lambda}_{n-1})}{\sum_{x_{n-1}=0}^1 \mathbb{P}[Y_n = y_n | X_{n-1} = x_{n-1}, X_n = 1] q_{x_{n-1}1} \exp(-x_{n-1} \tilde{\lambda}_{n-1})} \\
&=: g(y_n, \tilde{\lambda}_{n-1}). \tag{16}
\end{aligned}$$

Here, (a) follows by a recursive application of Bayes' Theorem and of the Markov property, whereas (b) exploits again the fact  $P(x_{n-1} | y^{n-1}) = P(x_{n-1} | \tilde{\lambda}_{n-1})$ , which holds true in the surrogate myopic model, and  $P(x_{n-1} | \tilde{\lambda}_{n-1}) \propto \exp(-x_{n-1} \tilde{\lambda}_{n-1})$ . We will see numerically that the recursion  $\tilde{\lambda}_n = g(y_n, \tilde{\lambda}_{n-1})$  yields estimates of the actual APP logarithmic ratio that are accurate enough to characterize the estimation entropy under the reactive transmission strategy with good approximation. Notably, the evaluation of the recursion  $\tilde{\lambda}_n = g(y_n, \tilde{\lambda}_{n-1})$  entails a complexity that is independent on the number of sources.

**Remark 3.** *It is worth mentioning that, as a consequence of Remark 1, the recursion (III-D1) yields the exact APP logarithmic ratio when the sources have symmetric transition probabilities, i.e., when  $q_{00} = q_{11}$ .*

#### IV. DENSITY EVOLUTION ANALYSIS

Recalling that the distribution of the estimation entropy  $H_n$  can be derived from the distribution of the APP logarithmic ratio  $\Lambda_n$  (using (III-B)), we consider next the problem of obtaining the distribution of the r.v.  $\Lambda_n$ . To do so, we employ a density evolution (DE) [29] approach to the recursive calculation of the APP logarithmic ratio density over the trellis diagram describing the evolution of the HMM state [30, Chapter 4]. We instantiate the analysis for both the random and the reactive transmission strategies. To numerically implement the analysis, we resort to quantized DE [46]. Note that in the reactive case, the analysis requires tracking the evolution of the joint distribution of a  $2M - 1$  random variables,

rendering the quantized DE analysis intractable even under simple quantization rules. For this reason, we will resort only to the myopic state estimator.

#### A. Random Transmission Strategy

The analysis is based on a recursive calculation of the distribution of  $\Lambda_n$  given the distributions of  $\Lambda_{n-1}$  and of  $Y_n|X_n$ . Suppose the joint distribution of  $\Lambda_{n-1}$  and  $X_{n-1}$  to be known. We have that

$$\begin{aligned}
 P(\lambda_n, x_n) &= \sum_{x_{n-1}=0}^1 \sum_{\substack{y_n, \lambda_{n-1}: \\ f(y_n, \lambda_{n-1})=\lambda_n}} P(\lambda_{n-1}, y_n, x_n, x_{n-1}) \\
 &= \sum_{x_{n-1}=0}^1 \sum_{\substack{y_n, \lambda_{n-1}: \\ f(y_n, \lambda_{n-1})=\lambda_n}} P(y_n|x_n, x_{n-1})P(x_n|x_{n-1})P(\lambda_{n-1}, x_{n-1}) \\
 &= \sum_{\substack{y_n, \lambda_{n-1}: \\ f(y_n, \lambda_{n-1})=\lambda_n}} P(y_n|x_n) \sum_{x_{n-1}=0}^1 P(x_n|x_{n-1})P(\lambda_{n-1}, x_{n-1})
 \end{aligned} \tag{17}$$

where  $f(y_n, \lambda_{n-1})$  is given in (III-C), which readily provides the evolution of the joint distribution. The recursion is initialized by assuming no initial knowledge on the state, i.e., by setting  $P[\Lambda_{-1} = 0, X_{-1} = 0] = P[\Lambda_{-1} = 0, X_{-1} = 1] = 1/2$ .

#### B. Reactive Transmission Strategy

We consider the myopic estimator, under the surrogate myopic model introduced in Section III-D1. Also in this case the analysis is based on a recursive calculation of the distribution of  $\tilde{\Lambda}_n$  given the distributions of  $\tilde{\Lambda}_{n-1}$  and of  $Y_n|X_n, X_{n-1}$ . Suppose the joint distribution of  $\tilde{\Lambda}_{n-1}$  and  $X_{n-1}$  to be known. We have that

$$\begin{aligned}
 P(\tilde{\lambda}_n, x_n) &= \sum_{x_{n-1}=0}^1 \sum_{\substack{y_n, \tilde{\lambda}_{n-1}: \\ g(y_n, \tilde{\lambda}_{n-1})=\tilde{\lambda}_n}} P(\tilde{\lambda}_{n-1}, y_n, x_n, x_{n-1}) \\
 &= \sum_{x_{n-1}=0}^1 \sum_{\substack{y_n, \tilde{\lambda}_{n-1}: \\ g(y_n, \tilde{\lambda}_{n-1})=\tilde{\lambda}_n}} P(y_n|x_n, x_{n-1})P(x_n|x_{n-1})P(\tilde{\lambda}_{n-1}, x_{n-1})
 \end{aligned} \tag{18}$$

where  $g(y_n, \tilde{\lambda}_{n-1})$  is given in (III-D1), which provides the evolution of the joint distribution. The recursion is initialized by setting  $P[\tilde{\Lambda}_{-1} = 0, X_{-1} = 0] = P[\tilde{\Lambda}_{-1} = 0, X_{-1} = 1] = 1/2$ .

## V. PRAGMATIC STATE ESTIMATION: DECODE&HOLD

The approach presented in Sec. III provides the receiver with an optimal estimate of the current source state, minimizing the probability of error. The complexity entailed by running a MAP estimator may however be critical in many settings, e.g., when messages are delivered to a battery-powered and computationally-limited collector [2], [47]. For such scenarios, other detectors may be preferred, trading off an optimal estimate in favor of a simpler implementation.

Starting from this remark, we consider in this section an alternative solution, based on a *decode and hold* (D&H) estimator. Following this approach, the receiver maintains at any time  $n$  an estimate  $\hat{X}_n$  for the reference source, which is updated whenever a packet is decoded and reveals the current state of the node of interest, or remains unchanged otherwise. More formally:

$$\hat{X}_n = \begin{cases} Y_n & \text{if } Y_n \in \{0, 1\} \\ \hat{X}_{n-1} & \text{if } Y_n \in \{\mathbf{I}, \mathbf{C}, \ominus, \oplus\}. \end{cases} \quad (19)$$

As highlighted in (V), the D&H solution does not trigger the calculations of an APP logarithmic ratio required by the MAP estimator. On the other hand, the following example provides an intuition of why the simple scheme is inherently suboptimal.

**Example 3.** Consider the case of a system with  $M = 2$  sources, operating under the reactive transmission strategy, and assume the following evolution:

- at time  $n - 2$ , we have  $X_{n-2} = 0$ ,  $X_{n-2}^{(1)} = 1$
- at time  $n - 1$  only the source of interest transitions:  $X_{n-1} = 1$ ,  $X_{n-1}^{(1)} = 1$
- at time  $n$  both sources transition:  $X_n = 0$ ,  $X_n^{(1)} = 0$

Accordingly, slot  $n - 1$  sees the sole transmission of the reference source, so that  $Y_{n-1} = 1$ , whereas a collision is experienced over slot  $n$ , i.e.  $Y_n = \mathbf{C}$ . In this situation, the D&H estimator outputs the sequence  $\hat{X}_{n-1} = 1$ ,  $\hat{X}_n = 1$ , providing an erroneous estimate in slot  $n$  (i.e.,  $\hat{X}_n \neq X_n$ ). Conversely, the output of the threshold test on the APP logarithmic ratio in (III) performed by the MAP approach returns the correct estimates in both time instants. This can readily be verified by observing that, for the case under study,  $\mathbb{P}[X_n = 0 \mid Y_n = \mathbf{C}, Y_{n-1} = 1, Y^{n-2} = y^{n-2}] = 1$ . Indeed, the observation of a collision implies that both nodes transmitted, and hence changed their state, providing certain knowledge of the state of the reference source at time  $n$  as well. The suboptimality of the D&H estimator stems by disregarding this type of information.

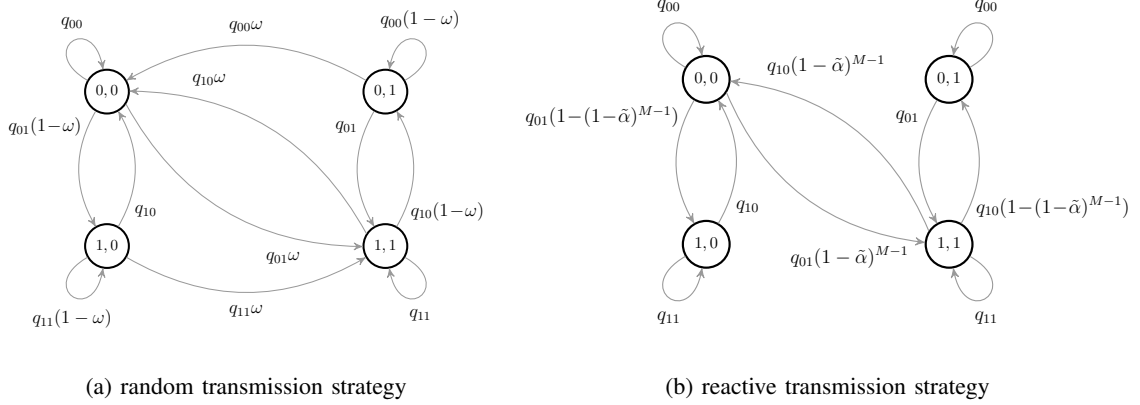


Fig. 6. Markov chains  $(X_n, \hat{X}_n)$  tracking the evolution of reference source state and D&H estimate, in the case of a random (a) and reactive (b) transmission policy.

To characterize the performance of this low-complexity solution, we focus on the average error probability  $P_e$ , which can be effectively computed by jointly tracking the source state and estimate processes via the Markov chain  $(X_n, \hat{X}_n)$ . The analysis we present is exact under random transmissions, whereas it resorts to the myopic surrogate model when the reactive strategy is implemented.

Let us first focus on the random approach. In this case, the transition probabilities of the chain are summarized in Fig. 6a, where we recall that  $\omega = \alpha(1-\alpha)^{M-1}$  is the probability that a node successfully delivers an update over a slot. As an example, consider state  $(X_n, \hat{X}_n) = (0, 0)$ . The process remains in the same state over the next slot if no change of state occurs, i.e. with probability  $q_{00}$ . Note indeed that  $\hat{X}_{n+1}$  will remain 0 both in case of transmission and successful delivery of an update (i.e.  $Y_{n+1} = 0$ ), and in the absence of a received packet from the reference source (i.e.  $Y_{n+1} \in \{\mathbf{I}, \mathbf{C}, \ominus, \oplus\}$ ). Instead, no transition to state  $(0, 1)$  can take place, since the D&H estimator would only reset  $\hat{X}_{n+1}$  to 1 upon receiving an update from the source containing that value, which is not possible when  $X_{n+1} = 0$ . In turn, the system moves to  $(1, 0)$  – providing an erroneous estimate of the source state – whenever the node of interest changes state (probability  $q_{01}$ ) but does not deliver an update, either due to a collision or for lack of transmission (overall probability  $1 - \omega$ ). Conversely, a transition to  $(1, 1)$  occurs when the source moves to state 1 and successfully sends a packet in slot  $n + 1$  (probability  $q_{01}\omega$ ). All other probabilities in the chain can be derived following a similar reasoning.

The finite state Markov process is readily shown to be aperiodic and irreducible, and thus ergodic. Accordingly, the error probability  $P_e$  introduced in (II-D), expressing the average

time spent by the chain in  $(0, 1)$  and  $(1, 0)$ , can be computed as the sum of the stationary probabilities of such states, denoted by  $\pi_{(0,1)}$  and  $\pi_{(1,0)}$ . Solving the balance equation, we get

$$P_e = \pi_{(0,1)} + \pi_{(1,0)} = \frac{2q_{01}q_{10}(1-\omega)}{(q_{01} + q_{10})[\omega + (1-\omega)(q_{01} + q_{10})]}. \quad (20)$$

The same approach can be leveraged to derive the performance of the D&H estimator when the nodes operate following a reactive transmission policy, leaning on the surrogate myopic model introduced in Sec. III-D1. The corresponding transition probabilities for the Markov chain  $(X_n, \hat{X}_n)$  take the form reported in Fig. 6b. In this case, the term  $(1 - \tilde{\alpha})^{M-1}$  captures the probability for a source to deliver an update over a slot once a state change has taken place, with the activation probability  $\tilde{\alpha}$  defined in (II-C). The stationary distribution of the chain gives in this case

$$\pi_{(0,1)} \approx \frac{q_{10}(1 - (1 - \tilde{\alpha})^{M-1})}{(q_{01} + q_{10})(2 - (1 - \tilde{\alpha})^{M-1})}, \quad \pi_{(1,0)} \approx \frac{q_{01}(1 - (1 - \tilde{\alpha})^{M-1})}{(q_{01} + q_{10})(2 - (1 - \tilde{\alpha})^{M-1})}$$

leading to an average error probability

$$P_e \approx \frac{1 - (1 - \tilde{\alpha})^{M-1}}{2 - (1 - \tilde{\alpha})^{M-1}}. \quad (21)$$

As discussed, this is exact for symmetric sources (i.e.  $q_{01} = q_{10}$ ), whereas it is only an approximation in the asymmetric case.

First insights on the behavior of the D&H estimator are offered by Fig. 7, which reports  $P_e$  against the number of nodes in the network in the case of symmetric sources ( $q_{01} = q_{10} = 0.01$ ). Blue lines refer to performance attained under the random transmission policy, whereas red ones are representative of the reactive approach. In the former case, the activation probability has been set as the reciprocal of the number of nodes, i.e.,  $\alpha = 1/M$ , in order to maximize the throughput and thus the average number of delivered updates. In the plot, solid lines report the analytical results for the D&H estimator obtained via (V) and (V), whereas circle markers denote the results of Monte Carlo simulations. Finally, dashed lines show the performance of a MAP estimator, which can be derived from the DE analysis. In particular, for the random transmission strategy case the error probability is

$$P_e = \lim_{n \rightarrow \infty} \sum_{\lambda_n \leq 0} P(\lambda_n, 0) + \lim_{n \rightarrow \infty} \sum_{\lambda_n > 0} P(\lambda_n, 1) \quad (22)$$

where  $P(\lambda_n, x_n)$  is computed with the recursion (IV-A). Note that to practically estimate the limit in (V) it suffices to let  $n$  grow large enough (e.g.,  $n \approx 10^5$ ) to observe converging

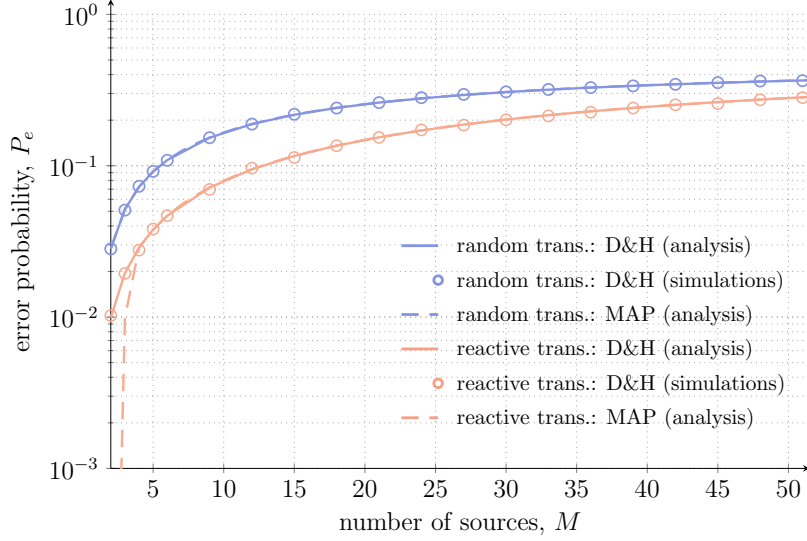


Fig. 7. Average state estimate error probability,  $P_e$ , against the number of devices in the network, symmetric source case ( $q_{10} = q_{01} = 0.01$ ). Solid lines denote analytical results for the D&H estimator, whereas circle markers the outcome of Monte Carlo simulations. Dashed lines report results for a MAP estimator using (V) and (V). Different colors indicate the performance attained under the random (blue) or reactive (red) transmission policy.

probability estimates. Similarly, the error probability for the MAP estimator for the reactive transmission strategy case can be obtained, in the myopic approximation setting, as

$$P_e \approx \lim_{n \rightarrow \infty} \sum_{\tilde{\lambda}_n \leq 0} P(\tilde{\lambda}_n, 0) + \lim_{n \rightarrow \infty} \sum_{\tilde{\lambda}_n > 0} P(\tilde{\lambda}_n, 1) \quad (23)$$

where  $P(\tilde{\lambda}_n, x_n)$  follows from the DE recursion (IV-B).

The reported trends pinpoint a visible gap between the two estimators when few nodes populate the network. The rationale behind this goes along the lines of the discussion presented in Example 2. Indeed, while both MAP and D&H attain an exact knowledge whenever a packet from the tracked source is received, the former refines its estimate also in the presence of an idle slot, a collision, or upon receiving a packet from another node ( $Y_n \in \{\mathbf{I}, \mathbf{C}, \ominus, \oplus\}$ ). Such side information is especially beneficial for low values of  $M$ , as it allows to infer with a good level of confidence the state of the reference process. A simple quantitative intuition on this can be grasped by focusing on the reactive strategy and by considering the likelihood ratio

$$\frac{P[X_n = X_{n-1}, Y_n = \mathbf{C}]}{P[X_n \neq X_{n-1}, Y_n = \mathbf{C}]} = \frac{(1 - \alpha) [1 - (1 - \alpha)^{M-1} - (M - 1)(1 - \alpha)^{M-2}]}{\alpha [1 - (1 - \alpha)^{M-1}]} \quad (24)$$

obtained in the event of a collision and only looking at the outcome of the last slot. The quantity evaluates to 0 for  $M = 2$ , allowing the MAP estimator to extract exact knowledge

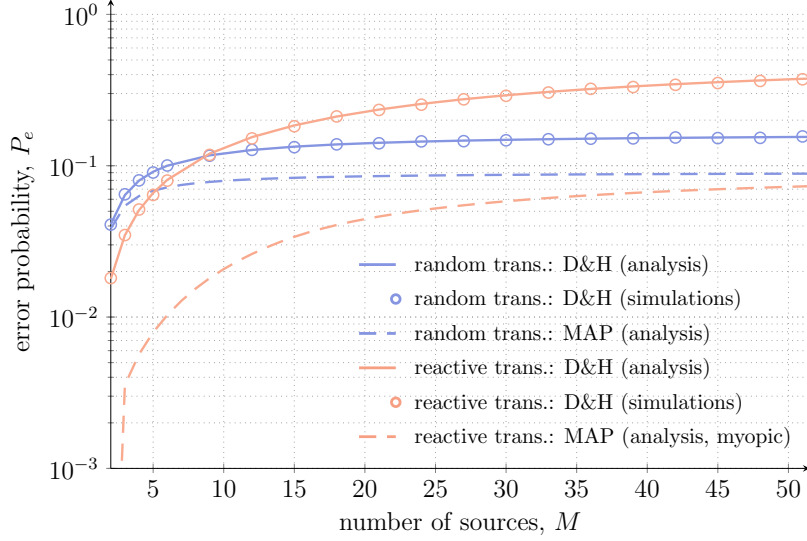


Fig. 8. Average state estimate error probability,  $P_e$ , against the number of devices in the network, asymmetric source case ( $q_{10} = 0.01, q_{01} = 0.1$ ). Solid lines denote analytical results for the D&H estimator, whereas circle markers the outcome of Monte Carlo simulations. Dashed lines report results for a MAP estimator obtained via (V) and (V) (myopic surrogate). Different colors indicate the performance attained under the random (blue) or reactive (red) transmission policy.

on the change of state, as discussed in the previously presented example. Interestingly, the performance gap between the two approaches vanishes as the number of sources increases. For larger  $M$ , indeed, idle slots occur more seldom, and the impact of observing a collision on the MAP estimate of the reference source becomes weaker. A hint on this is again offered for the reactive case by (V), as the likelihood ratio converges to  $(1 - \alpha)/\alpha$  for  $M \rightarrow \infty$ . This observation is of practical relevance, suggesting that the simple D&H solution offers good performance in sufficiently large networks when symmetric sources are to be tracked.

Fig. 7 also reveals that a lower error probability is attained for the configuration under study when nodes implement a reactive transmission approach, especially for low to intermediate values of  $M$ . The choice of accessing the channel only to signal a change of state is in this case particularly beneficial, increasing the probability of successfully notifying an update. Conversely, when sources are sampled at random times, nodes may attempt to report information which is already available at the receiver, congesting the medium unnecessarily and generating additional collisions that reduce the estimator accuracy.

These remarks are complemented by Fig. 8, which shows the same set of performance trends in the case of asymmetric sources, assuming  $q_{01} = 0.01, q_{10} = 0.1$ . Within the plot, let us first consider the behavior observed when the reactive policy is implemented (red lines).

In this case, simulation results show a very tight match with the analytical formulation of  $P_e$  for the D&H estimator (V), obtained relying on the myopic surrogate approximation. On the other hand, a significant gap is present with respect to the behavior of a MAP approach, for all values of  $M$ . This stems from the long time that may be required for an erroneous D&H estimate to be corrected. For the configuration under study, for instance, a change of the Markov chain  $(X_n, \hat{X}_n)$  in Fig. 6b from state  $(0, 1)$  to an exact knowledge can occur at the earliest when the source takes the less likely transition to state 1 and the transmitted update is correctly received (i.e.,  $(X_n, \hat{X}_n)$  transitions to  $(1, 1)$ , taking on average  $1/[q_{01}(1 - \tilde{\alpha})^{M-1}]$  slots). Conversely, the MAP approach can better refine its estimate at each slot, possibly correcting the erroneous knowledge without the need for the source to perform any further transmission.

In addition, and in contrast to what observed in the symmetric case, the D&H estimator performs worse when nodes implement a reactive rather than a random transmission policy, already for relatively low values of  $M$ . The trend can again be explained observing that in the former case the estimator can remain in error for a long time due to lack of transitions (and thus update transmissions) of the reference source. When delivery attempts are performed at random times, instead, such periods of drought can be shortened, with beneficial effects on the average error probability.

## VI. RESULTS AND DISCUSSION

We analyze the SEE as a function of the nodes' population size under both random and reactive transmission strategies. The results are obtained via DE analysis as reported in Sec. IV, and verified by means of Monte Carlo simulations. In the latter case, the entropy  $h(y^n)$  is tracked relying on a MAP estimator for each realization, and the SEE is estimated by averaging the results obtained for large values of  $n$ .

First insights on the behavior of the different access policies are provided in Fig. 9, which reports the average SEE against the number of sources  $M$  in the system for the symmetric case  $q_{01} = q_{10}$ . In the plot, blue lines refer to the random transmission approach, whereas red ones are relative to the reactive strategy. Solid and dashed patterns are used to distinguish results obtained for  $q_{01} = q_{10} = 0.1$  and  $q_{01} = q_{10} = 0.01$ , respectively.

For the random transmission strategy, the activation probability  $\alpha$  has been set to  $1/M$ . This choice maximizes the throughput of slotted ALOHA, and, as discussed in Sec. II-E, is also optimal in terms of average AoI. It is easy to observe that setting  $\alpha = 1/M$  minimizes the SEE, too. To see this, it is sufficient to note that the problem of estimating the state  $X_n$  given

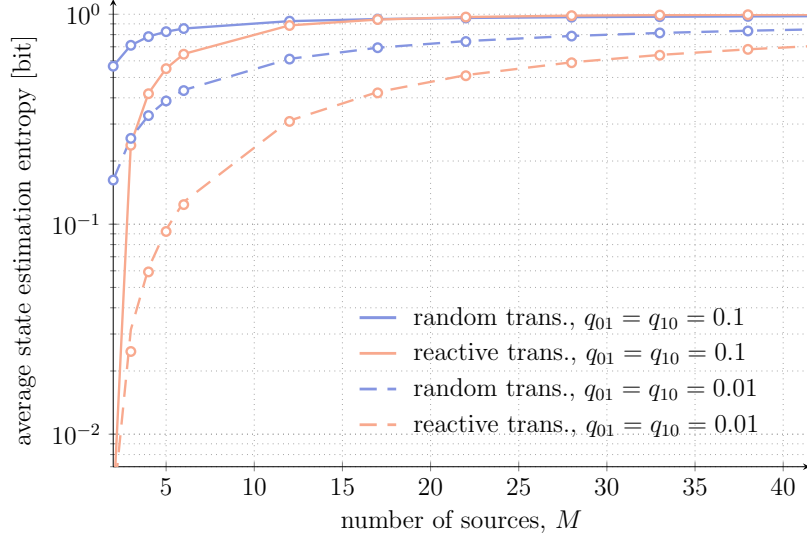


Fig. 9. Average SEE vs. number of nodes  $M$ , in the case of symmetric sources ( $q_{01} = q_{10}$ ). Lines denote results obtained via DE analysis, whereas markers the output of Monte Carlo simulations.

the observations  $Y^n$  is equivalent to the problem of estimating  $X_n$  with  $Y_0, Y_1, \dots, Y_n$  being the observations of  $X_0, X_1, \dots, X_n$  after transmission over  $n+1$  independent binary erasure channels (BECs) with erasure probability  $\epsilon = 1 - \omega$ , where the channel output alphabet is  $\{0, 1, ?\}$  and  $?$  denotes an erasure. The observation follows by the fact that, under random transmissions, observing  $Y_n \in \{I, C, \ominus, \oplus\}$  does not yield any information on  $X_n$ , hence any channel output in  $\{I, C, \ominus, \oplus\}$  can be regarded as an erasure. The conditional entropy  $H(X_n|Y^n)$  is hence minimized by minimizing  $\epsilon$ , i.e., by maximizing  $\omega = \alpha(1 - \alpha)^{M-1}$ .

Fig. 9 offers several take-aways. First, as expected, the average SEE raises in all cases when more nodes populate the network. The trend stems from the harsher channel contention experienced for larger values of  $M$ , which increases the probability of losing updates due to collisions and thus the uncertainty at the receiver. In contrast, lower values of the state transition probability  $q_{01} = q_{10}$  improve the SEE. The reason is twofold. On the one hand, when the source status changes less often, fewer updates are required on average at the receiver to track its evolution, and the loss of packets entail a lower increase in the uncertainty level. On the other hand, more sporadic transitions reduce the channel contention in the reactive case, increasing the probability of successfully delivering a packet and positively impacting the metric. The plot also pinpoints the beneficial effect of implementing a reactive transmission strategy. As discussed, having sources only notifying state changes helps preventing congestion, whereas a random transmission approach may see nodes occupy the

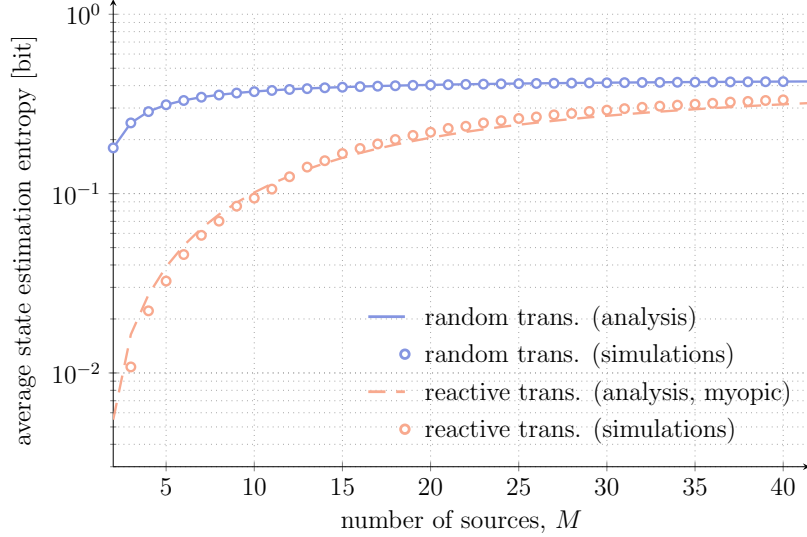


Fig. 10. Average SEE vs. number of nodes  $M$ . Asymmetric source case:  $q_{01} = 0.01$ ,  $q_{10} = 0.1$ . Lines denote results obtained via DE analysis, whereas markers the output of Monte Carlo simulations. For the reactive case, the myopic surrogate model was used for DE.

channel to send information already available at the receiver or, similarly, not promptly notify a relevant state modification. The effect is especially apparent for low values of  $M$ . Notably, for  $M = 2$ , perfect knowledge is available at the receiver for the reactive policy (SEE equal to 0). Indeed, in this case, once the state of both nodes is known, if a collision occurs the receiver deduces a simultaneous state change at the sources, which allows to know which the new states are.

The behavior in presence of asymmetric sources is reported in Fig. 10, considering  $q_{01} = 0.01$  and  $q_{10} = 0.1$ . In this case, we recall that the analytical results obtained via DE for the reactive transmission strategy offer an approximation, as they were derived resorting to the myopic surrogate model described in Sec. III-D1. Nonetheless, a very tight match can be observed with the results of Monte Carlo simulations, which estimate the average SEE taking into account the evolution of all sources in the systems. The outcome is particularly interesting, as it corroborates the accuracy of the proposed simplified analytical approach in capturing the behavior of the policy also for asymmetric transitions.

For the rest, the plot confirms the trends discussed in the symmetric case. From this standpoint, it is interesting to observe that the average SEE tends to converge for large values of  $M$  to the entropy of the stationary state distributions of the respective Markov chains, which is 1 for the symmetric case and  $\approx 0.44$  for the asymmetric one under study. In fact, as more nodes populate the system, the number of received packets per source progressively sinks

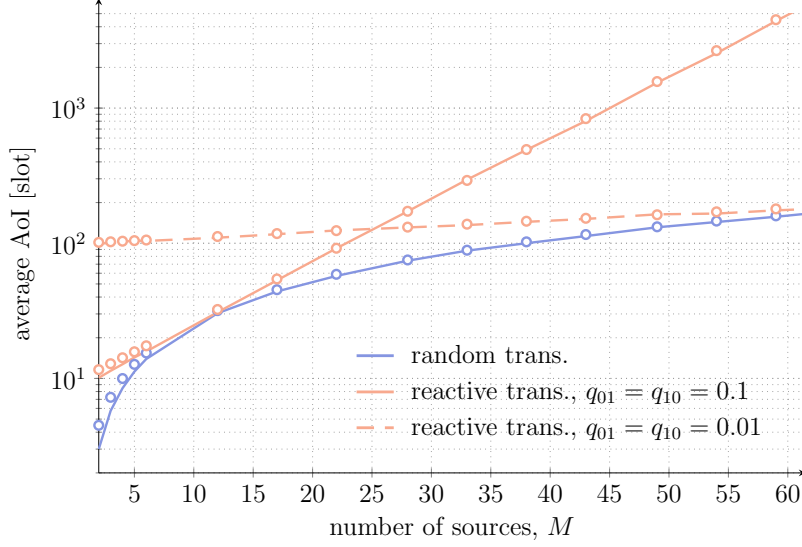


Fig. 11. Average AoI vs number of nodes  $M$ , in the case of symmetric sources. Lines denote results obtained analytically, whereas markers the output of Monte Carlo simulations. For the random strategy,  $\alpha = 1/M$ .

(either because of collisions, in the case of the reactive scheme, or because the activation probability falls to 0 asymptotically in  $M$  for the random scheme), reducing the amount of information available at the receiver on the tracked processes.

The results reported so far have highlighted the beneficial role played by a transmissions strategy that is tuned to the process being monitored, when aiming at maintaining a low SEE at the receiver in the presence of sources that are not memoryless. Such outcome is particularly interesting, as it suggests medium access control design principles that inherently differ from those commonly considered when targeting information freshness. To appreciate this, we explore the behavior of both the random and reactive transmission strategies in terms of average AoI. As discussed in Sec. II-E, the metric is commonly employed to capture how up to date the perception of a monitored process is at the receiver, and tracks the time elapsed since the generation of the last received update. In slotted ALOHA systems, AoI takes the form reported in (II-E), and is minimized by maximizing the average throughput, i.e., the frequency with which each source can successfully report data. From this standpoint, it is in fact important to observe that the metric is by definition oblivious of the actual value being delivered. In this sense, generating a reading and delivering it would lead to a reset of AoI, regardless of the actual content of the message.

The average AoI obtained for the access strategies under study is reported in Fig 11 against the number of nodes in the network, considering symmetric sources ( $q_{10} = q_{01} = 0.1$ , and  $q_{10} = q_{01} = 0.01$ ). For the random transmission,  $\alpha = 1/M$ , as already discussed. We

furthermore note that only one curve is reported for such approach, as its performance in terms of AoI does not depend on the transitions of the underlying monitored source. This is not the case for reactive transmissions, as the activation probability inherently depends on how frequently the sources transition. Focusing on the two curves for the reactive approach, we also note that, when few nodes are present, a higher transmission frequency ( $q_{01} = 0.1$ ) leads to lower AoI, as collisions are seldom experienced and updates can be delivered more often. Conversely, as  $M$  grows, the lower transmission rate induced by the setting  $q_{01} = 0.01$  becomes beneficial, avoiding excessive congestion.

More interestingly, the plot reveals that the average AoI attained with a random transmission strategy is always lower compared to the one offered by the reactive scheme. The only point in which the two strategies coincide corresponds to the situation in which the state transition probability coincides with the optimal activation probability (i.e.,  $\tilde{\alpha} = 1/q_{01} = 1/M$ , obtained for  $M = 10$  nodes for  $q_{01} = 0.1$  and  $M = 100$  nodes for  $q_{01} = 0.01$  - out of the plot axes).

Remarkably, then, AoI and SEE suggest the use of different access solutions. The intuition behind this peculiar behavior is that the calculation of the AoI treats all packets as equally informative. Hence, taking the stochastic model of the source into account (as in the reactive transmission strategy) does not provide any advantage. In this sense, it is important to observe that AoI can be an adequate metric in contexts where the fresh information is needed. However, when the actual state of a monitored process plays a major role, maintaining a low uncertainty level at the receiver may be critical. In this sense, the SEE naturally emerges as a good candidate metric, and the profoundly different hints it provides in terms of access strategy shall be taken into account in the design of the system.

## VII. CONCLUSIONS

In this paper, we have studied a system in which multiple terminals share a common slotted ALOHA channel to report updates towards a receiver. Assuming each node to monitor a two-state Markov source, we characterized the performance of the system in terms of average state estimation entropy, capturing the uncertainty at the receiver about the state of the tracked processes, under two transmission strategies: random and reactive. In the former case, a node randomly sends a status update at each slot, whereas in the latter a message is transmitted only if the monitored source has experienced a state change. We provided an analytical characterization of the SEE, and showed that its calculation is amenable to efficient implementation through DE, which allows to evaluate how the system performance

scales with the number of source nodes. Our study reveals that a reactive solution can offer better performance, lowering channel congestion and favoring delivery of relevant updates. Notably, this design hint differs from what suggested when considering the average AoI as reference metric, for which the random transmission approach is convenient. From this standpoint, AoI is an adequate metric in contexts where limited knowledge about the source statistics is available, and it is reasonable to assume that, the longer since the last update is received, the higher the uncertainty about the state of the source. However, in setups where the receiver has knowledge of the source model, other metrics that more accurately quantify the uncertainty of the receiver about the state of the sources are worth investigating. The SEE naturally emerges as a good candidate, as it captures the residual uncertainty on the state of the sources once the channel output and the source model have been taken into account.

## APPENDIX A

### CONDITIONAL STATISTICS OF CHANNEL OBSERVATIONS

In this appendix, we derive the statistical relation between the observed channel output at a generic slot,  $Y_n$ , and the state of the system sources, as introduced in the HMMs of Sec. III-A.

#### A. Random Transmission Strategy

For the transmission random policy, we are interested in computing the conditional distribution  $P(y_n|x_n)$  in (III-A1). We start by observing that, by the i.i.d. behavior of all nodes across slots, the channel output does not depend on the state of the reference source when  $Y_n \in \{\mathbf{I}, \mathbf{C}, \ominus, \oplus\}$ , i.e. in the case of idle slot, collision, or message reception from another node. Accordingly, we get

$$\left\{ \begin{array}{ll} \mathbb{P}[Y_n = \mathbf{I} | X_n = x_n] &= (1-\alpha)^M \\ \mathbb{P}[Y_n = \mathbf{C} | X_n = x_n] &= 1 - (1-\alpha)^M - M\omega \\ \mathbb{P}[Y_n = \ominus | X_n = x_n] &= (1-\alpha)(M-1)\pi_0\omega \\ \mathbb{P}[Y_n = \oplus | X_n = x_n] &= (1-\alpha)(M-1)\pi_1\omega \end{array} \right.$$

In particular, an idle slot is experienced when none of the  $M$  sources becomes active, whereas a collision when more than one node transmits. In turn, the probability of receiving a "one" or "zero" message from a source other than the reference one is obtained by jointly considering the event of having the reference source not transmitting  $(1-\alpha)$ , a single packet

sent over the slot by one of the other nodes (probability  $(M - 1)\omega$ ), and that the sender is in the corresponding state (probability  $\pi_0$  or  $\pi_1$ ).

Finally, the conditional probabilities when a packet from the reference source is received can be obtained as  $P[Y_n = 0 | X_n = 0] = P[Y_n = 1 | X_n = 1] = \omega$ ,  $P[Y_n = 0 | X_n = 1] = 0$ ,  $P[Y_n = 1 | X_n = 0] = 0$ . In the first case, the outcome is observed when the source transmits while all other contenders remain silent, whereas receiving a message from the source with a state different from the current one is not possible.

### B. Reactive Transmission Strategy, Symmetric Sources

When sources are symmetric ( $q_{01} = q_{10}$ ) and a reactive transmission strategy is employed, the corresponding HMM is fully characterized by specifying the conditional probabilities  $P(y_n | x_{n-1}, x_n)$ , as highlighted in (III-D1). Consider first the case  $Y_n = \mathbf{I}$ . Such an outcome can only be observed if the reference source does not transition (i.e.,  $X_{n-1} = X_n$ ) and the same holds for all other nodes. We thus get  $P[Y_n = \mathbf{I} | X_{n-1} = x_{n-1}, X_n = x_n] = (1 - \tilde{\alpha})^{M-1}$  for  $x_{n-1} = x_n$  and 0 otherwise. The reference source has to remain in the same state also for the receiver to retrieve a packet from any of the other nodes ( $Y_n \in \{\ominus, \oplus\}$ ). Accordingly,

$$\begin{aligned} P[Y_n = \ominus | X_{n-1} = x_{n-1}, X_n = x_{n-1}] &= P[Y_n = \oplus | X_{n-1} = x_{n-1}, X_n = x_{n-1}] \\ &= (M - 1) \frac{\tilde{\alpha}}{2} (1 - \tilde{\alpha})^{M-2} \end{aligned} \quad (25)$$

whereas  $P[Y_n = \ominus | X_{n-1} \neq X_n] = P[Y_n = \oplus | X_{n-1} \neq X_n] = 0$ . Within (A-B), the term  $\tilde{\alpha}/2 = \pi_0 q_{01} = \pi_1 q_{10}$  denotes the probability for one of the  $M - 1$  sources to perform the transition which is successfully reported to the receiver.

Similarly, when considering a collision outcome, the cases in which a state change (i.e., transmission) for the reference source takes place or not have to be distinguished. In the former, the activation of one or more of the remaining  $M - 1$  nodes suffices to have  $Y_n = \mathbf{C}$ , whereas two or more have to change state if the reference node does not. Following this reasoning we obtain

$$P[Y_n = \mathbf{C} | X_{n-1} = x_{n-1}, X_n = x_n] = \begin{cases} 1 - (1 - \tilde{\alpha})^{M-1} & \text{if } x_{n-1} \neq x_n \\ 1 - (1 - \tilde{\alpha})^{M-1} - (M - 1) \tilde{\alpha} (1 - \tilde{\alpha})^{M-2} & \text{else} \end{cases}$$

Lastly, the conditional probability of observing a reading from the source of interest can be derived with the same reasoning applied in the random transmission case:

$$P[Y_n = 0 \mid X_{n-1} = x_{n-1}, X_n = x_n] = \begin{cases} (1 - \tilde{\alpha})^{M-1} & \text{if } x_{n-1} = 1, x_n = 0 \\ 0 & \text{else} \end{cases} \quad (26)$$

$$P[Y_n = 1 \mid X_{n-1} = x_{n-1}, X_n = x_n] = \begin{cases} (1 - \tilde{\alpha})^{M-1} & \text{if } x_{n-1} = 0, x_n = 1 \\ 0 & \text{else} \end{cases} \quad (27)$$

### C. Reactive Transmission Strategy, Asymmetric Sources

For the general case of asymmetric sources ( $q_{10} \neq q_{01}$ ), we are interested in computing both the one-step transition probabilities of the Markov chain  $\sigma_n = (X_n, S_n)$  and the conditional probabilities  $P(y_n \mid \sigma_{n-1}, \sigma_n)$ . Let us first consider the former. Recalling the independent behavior of the reference source, we readily get

$$P(\sigma_n \mid \sigma_{n-1}) = P(x_n \mid x_{n-1}) \cdot P(s_n \mid s_{n-1}).$$

Denote now for the sake of compactness as  $\bar{S}_n$  the r.v. describing the number of sources in state 1 at a generic slot  $n$ , i.e.

$$\bar{S}_n = M - 1 - S_n.$$

By simple combinatorial arguments, it follows that

$$P[S_n = s_{n-1} + k \mid S_{n-1} = s_{n-1}] = \sum_{\ell=0}^{\min\{s_{n-1}, \bar{s}_{n-1}k\}} \binom{s_{n-1}}{\ell} q_{01}^{\ell} q_{00}^{s_{n-1}-\ell} \cdot \binom{\bar{s}_{n-1}}{\ell+k} q_{10}^{\ell+k} q_{11}^{\bar{s}_{n-1}-\ell-k}$$

for any  $0 \leq k \leq M - 1 - s_{n-1}$ . The expression accounts for all the possible cases in which the number of sources transitioning from state 1 to 0 is  $k$  more than those changing from 0 to 1. Similarly, when the number of sources in state 0 experiences an overall decrease, we obtain for any  $1 < k \leq s_{n-1}$

$$P[S_n = s_{n-1} - k \mid S_{n-1} = s_{n-1}] = \sum_{\ell=1}^{\min\{s_{n-1}-k, \bar{s}_{n-1}\}} \binom{s_{n-1}}{\ell} q_{01}^{\ell} q_{00}^{s_{n-1}-\ell} \cdot \binom{\bar{s}_{n-1}}{\ell-k} q_{10}^{\ell-k} q_{11}^{\bar{s}_{n-1}-\ell+k}.$$

Leaning on this, the conditional probabilities of observing  $Y_n$  can be derived. Consider first the case  $Y_n = 1$ . Recalling that an idle slot under the reactive strategy occurs only when

neither the reference source nor any of the other nodes transition, we get for  $S_n = S_{n-1}$  and  $X_n = X_{n-1}$

$$P[Y_n = \text{I} | \sigma_{n-1} = (x_{n-1}, s_{n-1}), \sigma_n = \sigma_{n-1}] = \frac{q_{00}^{s_{n-1}} q_{11}^{\bar{s}_{n-1}}}{P[S_n = s_{n-1} | S_{n-1} = s_{n-1}]} \quad (28)$$

and  $P[Y_n = \text{I} | \sigma_{n-1} = (x_{n-1}, s_{n-1}), \sigma_n = (x_n, s_n)] = 0$  otherwise. In (A-C), only the cases in which none of the other sources change state (probability  $q_{00}^{s_{n-1}} q_{11}^{\bar{s}_{n-1}}$ ) are accounted for in triggering an idle slot, as the overall event  $S_n = S_{n-1}$  also includes all cases in which the same number of nodes transitions from 0 to 1 and from 1 to 0. Following a similar reasoning, the conditional probabilities for the receiver to decode a packer from a source different from the reference one follow. Specifically, for  $S_n = S_{n-1} - 1$  and  $X_n = X_{n-1}$

$$P[Y_n = \oplus | \sigma_{n-1} = (x_{n-1}, s_{n-1}), \sigma_n = (x_{n-1}, s_{n-1} - 1)] = \frac{s_{n-1} q_{01} q_{00}^{s_{n-1}-1} q_{11}^{\bar{s}_{n-1}-1}}{P[S_n = s_{n-1} - 1 | S_{n-1} = s_{n-1}]}$$

and, for  $S_n = S_{n-1} + 1$ ,  $X_n = X_{n-1}$

$$P[Y_n = \ominus | \sigma_{n-1} = (x_{n-1}, s_{n-1}), \sigma_n = (x_{n-1}, s_{n-1} + 1)] = \frac{\bar{s}_{n-1} q_{10} q_{11}^{\bar{s}_{n-1}-1} q_{00}^{s_{n-1}}}{P[S_n = s_{n-1} + 1 | S_{n-1} = s_{n-1}]}.$$

In all other cases, the events cannot be observed. The expressions capture the event that only one of the sources performs a transition and notifies its new state.

Finally, the conditional probabilities for  $Y_n$  to take value 0 or 1 are akin to those obtained in (A-B), (A-B), as only the reference node has to transition over slot  $n$ . In this case, accounting for the asymmetry of the other sources, we have for  $S_n = S_{n-1}$  and  $X_n = 1$ ,  $X_{n-1} = 0$

$$P[Y_n = 1 | \sigma_{n-1} = (0, s_{n-1}), \sigma_n = (1, s_{n-1})] = \frac{q_{11}^{s_{n-1}} q_{00}^{\bar{s}_{n-1}}}{P[S_n = s_{n-1} | S_{n-1} = s_{n-1}]}$$

and  $P[Y_n = 1 | \sigma_{n-1} = (x_{n-1}, s_{n-1}), \sigma_n = (x_n, s_n)] = 0$  otherwise. Similarly

$$P[Y_n = 0 | \sigma_{n-1} = (1, s_{n-1}), \sigma_n = (0, s_{n-1})] = \frac{q_{11}^{s_{n-1}} q_{00}^{\bar{s}_{n-1}}}{P[S_n = s_{n-1} | S_{n-1} = s_{n-1}]}$$

and 0 otherwise.

In conclusion, the observation of a collision is the complementary event to those just described, and the corresponding probability, i.e.  $P[Y_n = \text{C} | \sigma_{n-1} = (x_{n-1}, s_{n-1}), \sigma_n = (x_n, s_n)]$  can be derived accordingly.

## REFERENCES

- [1] N. Abramson, "The throughput of packet broadcasting channels," *IEEE Trans. Commun.*, vol. COM-25, no. 1, pp. 117–128, 1977.
- [2] LoRa Alliance, "The LoRa Alliance Wide Area Networks for Internet of Things," [www.lora-alliance.org](http://www.lora-alliance.org).
- [3] S. Kaul, R. Yates, and M. Gruteser, "On piggybacking in vehicular networks," in *Proc. IEEE Globecom*, Dec. 2011.
- [4] —, "Real-time status: How often should one update?" in *Proc. IEEE INFOCOM*, Mar. 2012.
- [5] R. D. Yates, Y. Sun, D. R. Brown, S. K. Kaul, E. Modiano, and S. Ulukus, "Age of information: An introduction and survey," *IEEE J. Sel. Areas Commun.*, vol. 39, no. 5, pp. 1183–1210, 2021.
- [6] M. Costa, M. Codreanu, and A. Ephremides, "On the age of information in status update systems with packet management," *IEEE Trans. Inf. Theory*, vol. 62, no. 4, pp. 1897–1910, 2016.
- [7] E. Najm, R. Yates, and E. Soljanin, "Status updates through M/G/1/1 queues with HARQ," in *Proc. IEEE ISIT*, Jun. 2017.
- [8] R. Devassy, G. Durisi, G. C. Ferrante, O. Simeone, and E. Uysal, "Reliable transmission of short packets through queues and noisy channels under latency and peak-age violation guarantees," *IEEE J. Sel. Areas Commun.*, vol. 37, no. 4, pp. 721–734, 2019.
- [9] Y. Sun, Y. Polyanskiy, and E. Uysal, "Sampling of the Wiener process for remote estimation over a channel with random delay," *IEEE Trans. Inf. Theory*, vol. 66, no. 2, pp. 1118–1135, 2020.
- [10] E. Najm, R. Nasser, and E. Telatar, "Content based status updates," *IEEE Trans. Inf. Theory*, vol. 66, no. 6, pp. 3846–3863, 2020.
- [11] R. D. Yates, "The age of information in networks: Moments, distributions, and sampling," *IEEE Trans. Inf. Theory*, vol. 66, no. 9, pp. 5712–5728, 2020.
- [12] R. D. Yates and S. K. Kaul, "The age of information: Real-time status updating by multiple sources," *IEEE Trans. Inf. Theory*, vol. 65, no. 3, pp. 1807–1827, 2019.
- [13] I. Kadota, A. Sinha, and E. Modiano, "Scheduling algorithms for optimizing age of information in wireless networks with throughput constraints," *IEEE/ACM Trans. Netw.*, vol. 27, no. 4, pp. 1359–1372, 2019.
- [14] A. Kosta, N. Pappas, A. Ephremides, and V. Angelakis, "Age of information performance of multiaccess strategies with packet management," *Journal of Communications and Networks*, vol. 21, no. 3, pp. 244–255, 2019.
- [15] A. Maatouk, M. Assaad, and A. Ephremides, "Minimizing the age of information: NOMA or OMA?" in *Proc. IEEE INFOCOM Workshops*, Apr. 2019.
- [16] —, "On the age of information in a CSMA environment," *IEEE/ACM Trans. Netw.*, vol. 28, no. 2, pp. 818–831, 2020.
- [17] R. Yates and S. K. Kaul, "Status updates over unreliable multiaccess channels," in *Proc. IEEE ISIT*, Jun. 2017.
- [18] R. Yates and S. Kaul, "Age of information in uncoordinated unslotted updating," in *Proc. IEEE ISIT*, Jun. 2020.
- [19] O. T. Yavaskan and E. Uysal, "Analysis of slotted ALOHA with an age threshold," *IEEE J. Sel. Areas Commun.*, vol. 39, no. 5, 2021.
- [20] X. Chen, K. Gatsis, H. Hassani, and S. S. Bidokhti, "Age of information in random access channels," *IEEE Trans. Inf. Theory*, vol. 68, no. 10, pp. 6548–6568, 2022.
- [21] A. Maatouk, S. Kriouile, M. Assaad, and A. Ephremides, "The age of incorrect information: A new performance metric for status updates," *IEEE/ACM Trans. Netw.*, vol. 28, no. 5, pp. 2215–2228, 2020.
- [22] T. Soleymani, J. Baras, and S. Hirche, "Value of information in feedback control: Quantification," *IEEE Trans. Autom. Control*, vol. 67, no. 7, pp. 3730–3737, 2020.
- [23] M. Rezaeian, B.-N. Vo, and J. S. Evans, "The optimal observability of partially observable Markov decision processes: Discrete state space," *IEEE Trans. Autom. Control*, vol. 55, no. 12, pp. 2793–2798, 2010.

- [24] G. Chen, S. C. Liew, and Y. Shao, "Uncertainty-of-information scheduling: A restless multiarmed bandit framework," *IEEE Trans. Inf. Theory*, vol. 68, no. 9, pp. 6151–6173, 2022.
- [25] G. Chen and S. C. Liew, "An index policy for minimizing the uncertainty-of-information of Markov sources," 2022. [Online]. Available: <https://arxiv.org/abs/2212.02752v1>
- [26] G. Cocco, A. Munari, and G. Liva, "State estimation entropy for two-state Markov sources in slotted ALOHA random access channels," in *Proc. IEEE Info. Theo. Workshop (ITW)*, Apr. 23-28 2023.
- [27] S. Kaul, R. Yates, and M. Gruteser, "Real-time status: How often should one update?" in *Proc. IEEE INFOCOM*, Mar. 2012.
- [28] R. D. Yates and S. K. Kaul, "The age of information: Real-time status updating by multiple sources," *IEEE Trans. Inf. Theory*, vol. 65, no. 3, pp. 1807–1827, 2019.
- [29] T. Richardson and R. Urbanke, "The capacity of low-density parity-check codes under message-passing decoding," *IEEE Trans. Inf. Theory*, vol. 47, no. 2, pp. 599–618, 2001.
- [30] H. D. Pfister, "On the capacity of finite state channels and the analysis of convolutional accumulate- $m$  codes," Ph.D. dissertation, University of California, San Diego, 2003.
- [31] X. Gao, E. Akyol, and T. Başar, "On remote estimation with multiple communication channels," in *Proc. American Control Conference (ACC)*, Jul. 2016.
- [32] M-Salimnejad, M. Kountouris, and N. Pappas, "Real-time remote reconstruction of a Markov source and actuation over wireless," 2023. [Online]. Available: <https://arxiv.org/abs/2302.01132v1>
- [33] A. Nayyar, T. Başar, D. Teneketzis, and V. V. Veeravalli, "Optimal strategies for communication and remote estimation with an energy harvesting sensor," *IEEE Trans. Autom. Control*, vol. 58, no. 9, pp. 2246–2260, 2013.
- [34] X. Chen, X. Liao, and S. S. Bidokhti, "Real-time sampling and estimation on random access channels: Age of information and beyond," in *Proc. IEEE INFOCOM*, May 2022.
- [35] M. Rezaeian, "Sensor scheduling for optimal observability using estimation entropy," in *Proc. IEEE PERCOM Workshops*, Mar. 2007.
- [36] —, "Hidden Markov process: A new representation, entropy rate and estimation entropy," 2006. [Online]. Available: <https://arxiv.org/abs/cs/0606114>
- [37] R. Ambrosino, B. Sinopoli, K. Poolla, and S. Sastry, "Optimal sensor density for remote estimation over wireless sensor networks," in *Proc. IEEE Allerton Conference on Communication, Control, and Computing*, Sep. 2008.
- [38] "On the entropy of a hidden markov process," *Theoretical Computer Science*, vol. 395, no. 2, pp. 203–219, 2008.
- [39] J. Luo and D. Guo, "On the entropy rate of hidden Markov processes observed through arbitrary memoryless channels," *IEEE Trans. on Info. Theory*, vol. 55, no. 4, pp. 1460–1467, 2009.
- [40] T. Cover and J. Thomas, *Elements of Information Theory*. John Wiley and Sons, 2006.
- [41] S. Kaul, M. Gruteser, V. Rai, and J. Kenney, "Minimizing age of information in vehicular networks," in *Proc. IEEE SECON*, June 2011.
- [42] A. Munari, "Modern random access: an age of information perspective on irregular repetition slotted ALOHA," *IEEE Trans. Commun.*, vol. 69, no. 6, pp. 3572 – 3585, 2021.
- [43] T. Richardson and R. Urbanke, *Modern coding theory*. Cambridge University Press, 2008.
- [44] L. Bahl, J. Cocke, F. Jelinek, and J. Raviv, "Optimal decoding of linear codes for minimizing symbol error rate (corresp.)," *IEEE Trans. Inf. Theory*, vol. 20, no. 2, pp. 284–287, 1974.
- [45] L. Rabiner, "A tutorial on hidden Markov models and selected applications in speech recognition," *Proc. IEEE*, vol. 77, no. 2, pp. 257–286, Feb. 1989.
- [46] H. Jin and T. Richardson, "A new fast density evolution," in *Proc. IEEE Information Theory Workshop*, Mar. 2006.
- [47] Y. Wang, X. Lin, A. Adhikary, A. Grovlen, Y. Sui, Y. Blankenship, J. Bergman, and H. Razaghi, "A primer on 3GPP narrowband internet of things," *IEEE Commun. Mag.*, vol. 55, no. 3, pp. 117–123, 2017.